MBoC | ARTICLE

Lysosomal membrane proteins LAMP1 and LIMP2 are segregated in the Golgi apparatus independently of their clathrin adaptor binding motif

Jason Ecard[a,b], Yen-Ling Lian[a], Séverine Divoux[a], Zelia Gouveia[a], Emmanuelle Vigne[b], Franck Perez[a,†] and Gaelle Boncompain[a,†,*]

[a]Dynamics of Intracellular Organization Laboratory, Institut Curie, PSL Research University, Sorbonne Université, Centre National de la Recherche Scientifique, UMR 144, 75005, Paris, France; [b]Large Molecules Research, Sanofi, 94400 Vitry-Sur-Seine, France

ABSTRACT **To reach the lysosome, lysosomal membrane proteins (LMPs) are translocated in the endoplasmic reticulum after synthesis and then transported to the Golgi apparatus. The existence of a direct transport from the Golgi apparatus to the endosomes but also of an indirect route through the plasma membrane has been described. Clathrin adaptor binding motifs contained in the cytosolic tail of LMPs have been described as key players in their intracellular trafficking. Here we used the RUSH assay to synchronize the biosynthetic transport of multiple LMPs. After exiting the Golgi apparatus, RUSH-synchronized LAMP1 was addressed to the cell surface both after overexpression or at endogenous level. Its YXXΦ motif was not involved in the transport from the Golgi apparatus to the plasma membrane but in its endocytosis. LAMP1 and LIMP2 were sorted from each other after reaching the Golgi apparatus. LIMP2 was incorporated in punctate structures for export from the Golgi apparatus from which LAMP1 is excluded. LIMP2-containing post-Golgi transport intermediates did not rely neither on its adaptor binding signal nor on its C-terminal cytoplasmic domain.**

SIGNIFICANCE STATEMENT

- Lysosomal membrane proteins (LMPs) are transported to the lysosome through the Golgi apparatus. Their mode of biosynthetic delivery remains controversial. How LMPs are segregated in the Golgi and which motifs are involved is unknown.
- Using synchronization of their transport, the authors showed that LAMP1 transits through the plasma membrane before reaching the lysosome. LAMP1, LAMP2, and LAP are not segregated in the Golgi, while LAMP1 and LIMP2 are.
- Mutations of their clathrin adaptor binding motifs suggest that they are not involved in the segregation and sorting of these LMPs at the Golgi apparatus.

Monitoring Editor
Michael Marks
Children's Hospital of Philadelphia

Received: Jul 3, 2023
Revised: Jan 9, 2024
Accepted: Jan 9, 2024

This article was published online ahead of print in MBoC in Press (http://www.molbiolcell.org/cgi/doi/10.1091/mbc.E23-06-0251) on January 17, 2024.

†These authors contributed equally to this work.

*Address correspondence to: Gaelle Boncompain (gaelle.boncompain@curie.fr).

Abbreviations used: CLEM, correlative light-electron microscopy; EGFP, enhanced green fluorescent protein; ER, endoplasmic reticulum; FP, fluorescent protein; LE/Lys., late endosomes and lysosomes; LMP, lysosomal membrane protein; MPR, mannose-6-phosphate receptors; RUSH, retention using selective hooks; SBP, streptavidin binding peptide; TGN, *Trans*-Golgi Network; TIRF, total internal fluorescence microscopy.

INTRODUCTION

Lysosomes are membrane-bound organelles ensuring multiple functions necessary to cellular homeostasis such as degradation of molecules. Lysosomal proteins include soluble luminal enzymes and membrane integral proteins. For their delivery to late endosomes and lysosomes (LE/Lys.), neosynthesized lysosomal membrane proteins (LMPs) are translocated into the endoplasmic reticulum (ER) and transported to the Golgi apparatus. From there, LMP can follow a direct Golgi-to-endosome transport route, referred to as the direct pathway. Alternatively, they can be targeted to the plasma membrane and reach the endosomes by endocytosis, this pathway being called the indirect pathway (Braulke and Bonifacino, 2009).

Lysosomal Integral Membrane Protein 2 (LIMP2) is a type III LMP, which spans the membrane twice. It functions as a receptor for the transport of the lysosomal enzyme β-cerebrosidase to lysosomes (Reczek *et al.*, 2007). In addition, LIMP2 potentially works as a lipid transporter (Kuronita *et al.*, 2002; Conrad *et al.*, 2017; Heybrock *et al.*, 2019). LIMP2 follows a direct pathway to reach LE/Lys after transiting through the Golgi apparatus (Vega *et al.*, 1991; Obermuller *et al.*, 2002). The [D/E]XXXL[L/I] signal (X referring to any amino acid) in its cytoplasmic tail was shown to bind clathrin adaptor complexes AP1, AP2, and AP3, but not AP4, and to be important for its trafficking (Vega *et al.*, 1991; Ogata and Fukuda, 1994; Sandoval and Bakke, 1994; Honing *et al.*, 1998; Le Borgne *et al.*, 1998; Fujita *et al.*, 1999; Sandoval *et al.*, 2000; Tabuchi *et al.*, 2000; Janvier *et al.*, 2003; Mattera *et al.*, 2011). LIMP2-AP1 interaction was proposed to mediate the incorporation of LIMP2 within clathrin-coated vesicles at the *trans*-Golgi Network (TGN) allowing its exit from the Golgi apparatus (Fujita *et al.*, 1999).

Lysosomal-Associated Membrane Protein 1 (LAMP1) trafficking pathway is more controversial. Depending on the cell model, LAMP1 was shown to appear at the cell surface during its transport in some studies (Lippincott-Schwartz and Fambrough, 1986, 1987; Furuno *et al.*, 1989b) but not in others (Green *et al.*, 1987; Akasaki *et al.*, 1995). These differences were imputed to variable LAMP1 expression levels. It was proposed that high LAMP1 expression would lead to an overflow of the direct pathway and to its appearance at the cell surface (Harter and Mellman, 1992). LAMP1 bears a GYXXΦ signal (Φ referring to a bulky hydrophobic amino acid) in its cytoplasmic tail, the mutation of which abolishes its trafficking to lysosomes and redirects LAMP1 to the plasma membrane (Williams and Fukuda, 1990; Hunziker *et al.*, 1991; Harter and Mellman, 1992; Guarnieri *et al.*, 1993; Honing and Hunziker, 1995). This signal was shown to bind AP1, AP2, and AP3 (Ohno *et al.*, 1995, 1996; Honing *et al.*, 1996; Le Borgne *et al.*, 1998; Dell'Angelica *et al.*, 1999). Although AP1 was proposed to participate in the Golgi export of LAMP1 (Honing *et al.*, 1996), LAMP1 still reaches lysosomes in AP1-depleted cells (Meyer *et al.*, 2000). LAMP1 has been detected in clathrin-coated pits at the plasma membrane by electron microscopy (Furuno *et al.*, 1989a). Its endocytosis is dependent on clathrin, dynamin, and AP2 (Janvier and Bonifacino, 2005). LAMP1 is overexposed at the cell surface in AP3-depleted cells due to an increased recycling, suggesting a role for AP3 in the targeting of LAMP1 from early endosomes to LE/Lys (Dell'Angelica *et al.*, 1999; Peden *et al.*, 2004).

Chen *et al.* (2017) synchronized the anterograde transport of rat LAMP1 using the Retention Using Selective Hooks (RUSH) system. Briefly, the tagging of the protein of interest with Streptavidin Binding Peptide (SBP) and the coexpression of an ER-resident streptavidin-tagged protein maintains the protein of interest in the ER until biotin is added to the medium (Boncompain *et al.*, 2012). Chen *et al.* (2017) have shown that RUSH-synchronized rat LAMP1 exits the Golgi apparatus in tubulovesicular compartments, which fuse with the plasma membrane. These tubulovesicular compartments also contained plasma membrane-fated proteins, such as the transferrin receptor and VSV-G. In addition, none of the four APs complexes (AP1-4) appeared to be necessary for LAMP1 export from the Golgi apparatus.

Here, we study the trafficking pathway of human LAMP1 using the RUSH system and we demonstrate that RUSH-synchronized LAMP1 follows an indirect pathway to the LE/Lys. independently of its adaptor binding signal. The synchronized transport of other LMPs was analyzed and compared with the transport pathway of LAMP1. Our results show that LAMP1 and LIMP2 are segregated and sorted in the Golgi apparatus, LIMP2 being incorporated into punctate structures before being exported from the Golgi apparatus. These LIMP2-containing post-Golgi transport intermediates were shown to be clathrin-free and to rely neither on its adaptor binding signal nor on its C-terminal cytoplasmic domain.

RESULTS

Newly synthesized LAMP1 is transported from the Golgi apparatus to the plasma membrane before reaching the lysosomes

The anterograde transport of newly synthesized human LAMP1 was analyzed using the RUSH system (Boncompain *et al.*, 2012). LAMP1 was fused to a SBP and a fluorescent protein in its luminal domain and transiently expressed in HeLa cells. In the absence of biotin, SBP-mCherry-LAMP1 was retained in the ER, thanks to the coexpression of the ER-resident Streptavidin-KDEL (Supplemental Figure S1a). Synchronous release of SBP-mCherry-LAMP1 was induced by addition of biotin. Thirty-five minutes after addition of biotin, SBP-mCherry-LAMP1 was detected in the Golgi apparatus as shown by the colocalization with the Golgi marker GM130. Two hours after addition of biotin, SBP-mCherry-LAMP1 reached the LE/Lys., as evidenced by the colocalization with LAMTOR4 (Supplemental Figure S1, a and b). An immunostaining on nonpermeabilized cells using an anti-GFP antibody revealed that newly synthesized SBP-EGFP-LAMP1 was detected at the plasma membrane 35 and 60 min after the addition of biotin (Figure 1a). Flow cytometry was used to monitor the appearance of SBP-EGFP-LAMP1 at the cell surface thanks to immunostaining with an anti-GFP antibody on nonpermeabilized cells. The presence of SBP-EGFP-LAMP1 at the cell surface 30 min after its release from the ER was confirmed, peaked after 45 min and then decreased to reach the basal level after 90 min. The basal level of SBP-EGFP-LAMP1 at the cell surface was assessed by the condition in which biotin was added at the time of transfection (no interaction between SBP and Streptavidin occurs; Figure 1b). The synchronization of the transport of SBP-EGFP-LAMP1 and its appearance at the cell surface were validated in the breast cancer cell line SUM159 and in the nontumorigenic RPE-1 cell line (Supplemental Figure S1, c–e).

To rule out that the appearance of LAMP1 at the cell surface is due to high expression, we engineered the LAMP1 locus using CRISPR/Cas9 to synchronize the anterograde transport of endogenous LAMP1. SUM159 cells were genome-edited to insert SBP and mCherry at the N-terminus of LAMP1 downstream of the signal peptide (Supplemental Figure S2a). A clonal population with homozygous insertion of SBP-mCherry in LAMP1 gene was then further transduced to express Str-KDEL, necessary for synchronization of transport using the RUSH assay (Supplemental Figure S2b). The transport of endogenously tagged LAMP1 (SBP-mCherry-LAMP1^{EN})

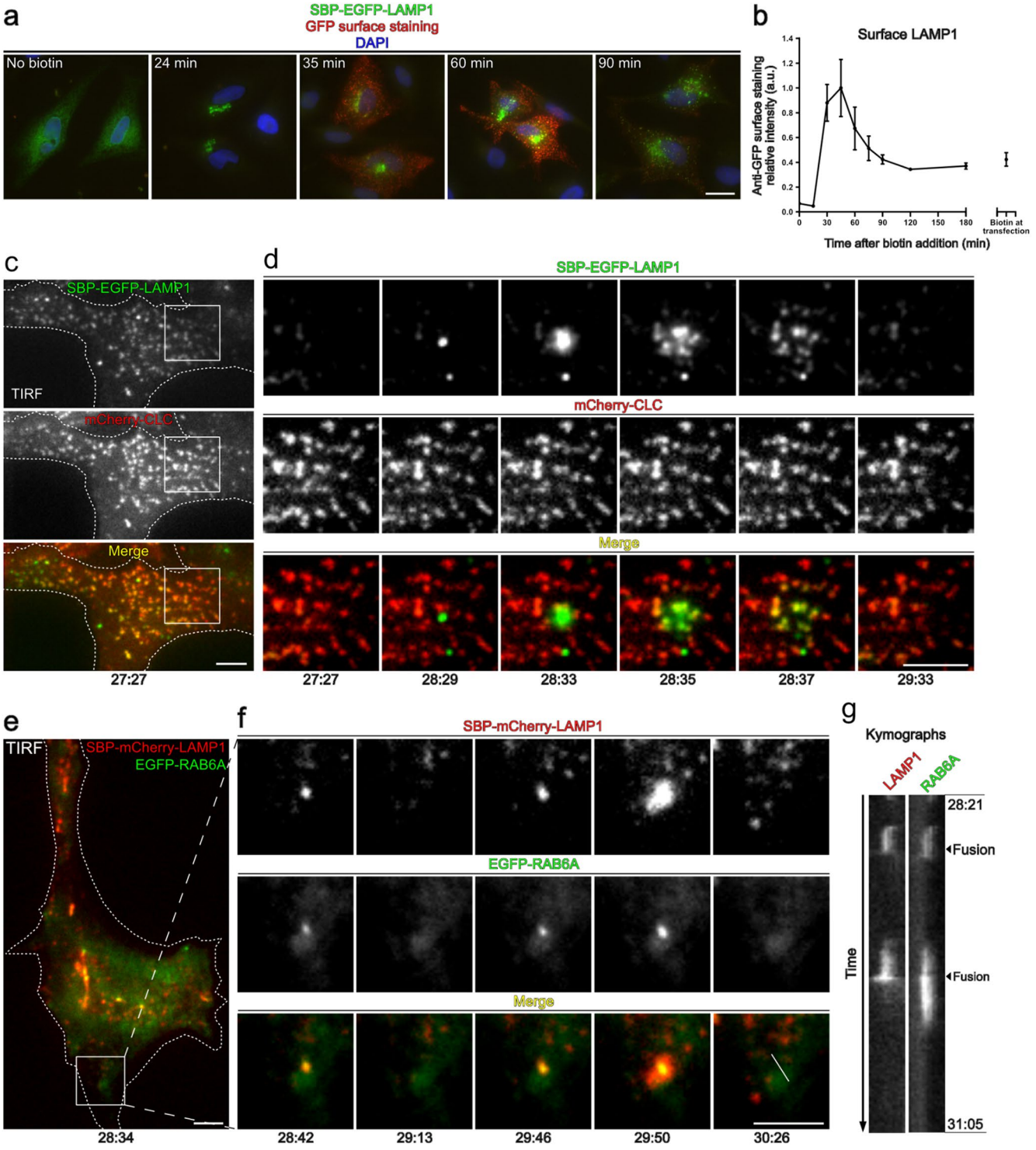

FIGURE 1: RUSH-synchronized LAMP1 is transported from the Golgi apparatus to the cell surface before being internalized from clathrin-coated pits. (a) Widefield microscopy images of HeLa cells transiently expressing SBP-EGFP-LAMP1 and Streptavidin-KDEL. Cells were incubated with biotin for the indicated times, stained with an anti-GFP antibody without permeabilization. Scale bar: 5 µm. (b) Flow cytometry measurement of the surface anti-GFP surface signal intensity of cells treated as in (a). Median anti-GFP intensity of GFP-positive cells normalized to the maximum value is shown. $n = 3$ independent experiments. Error bars: SEM. (c and d) TIRF images of living HeLa cells transiently expressing SBP-EGFP-LAMP1, Streptavidin-KDEL and mCherry-clathrin light chain (CLC) acquired at the indicated times after the addition of biotin. Scale bars: 5 µm. (d) Enlargement of the boxed area depicted in (c). (d) Time-lapse acquisition of a fusion event magnified from the boxed region in (c). (e and f) TIRF images of living HeLa cells transiently expressing SBP-mCherry-LAMP1, Streptavidin-KDEL and EGFP-RAB6A. Scale bars: 5 µm. (f) Fusion events magnified from the boxed region in (e). (g) Kymographs along the line in (f) between the two indicated times. Dotted lines highlight the cell contour. Time in min:s.

was efficiently synchronized from the ER to the lysosome upon addition of biotin (Supplemental Figure S2c). SBP-mCherry-LAMP1^{EN} was detected by flow cytometry and immunostaining with an anti-SBP antibody at the cell surface of nonpermeabilized cells 30 min after incubation with biotin, provided the ER hook was coexpressed (Supplemental Figure S2d).

Using Total Internal Reflection Fluorescence (TIRF) microscopy, fusion events of SBP-EGFP-LAMP1-containing carriers with the plasma membrane were observed (Figure 1, c and d; Supplemental Movie 1). Quickly after fusion has occurred, SBP-EGFP-LAMP1 was trapped in punctate structures, which are positive for mCherry-clathrin light chain indicating they might be clathrin-coated pits. The signal intensity of SBP-EGFP-LAMP1 in clathrin-coated pits then decreased suggesting its internalization through endocytosis. TIRF microscopy also showed that carriers containing LAMP1 and fusing with the plasma membrane were positive for RAB6 (Figure 1, e–g; Supplemental Movie 2). RAB6 is a Ras-related small GTPase involved in the regulation of trafficking pathways from the Golgi apparatus (Girod *et al.*, 1999; White *et al.*, 1999; Grigoriev *et al.*, 2007, 2011; Patwardhan *et al.*, 2017; Fourriere *et al.*, 2019). Previous studies have shown that RAB6 is a major regulator of the formation of post-Golgi carriers (Miserey-Lenkei *et al.*, 2010, 2017; Pereira *et al.*, 2023) and their delivery to the exocytic sites (Grigoriev *et al.*, 2011; Fourriere *et al.*, 2019).

Taken together, our results demonstrate that newly synthesized human LAMP1 is transported from the Golgi apparatus to the plasma membrane before being internalized via clathrin coated pits and transported to its final endosomal destination, LE/Lys.

Golgi-to-plasma membrane transport of LAMP1 is not dependent on its YXXΦ motif

The clathrin adaptor complexes AP1, AP2, AP3, and AP4 have been shown to recognize YXXΦ motifs in the cytosolic tail of proteins (Robinson, 2004). The motif $_{414}$YQTI$_{417}$ of LAMP1 (Figure 3a) was suggested to be involved in its direct Golgi-to-endosome transport pathway (Honing *et al.*, 1996; Obermuller *et al.*, 2002; Cook *et al.*, 2004). We mutated the LAMP1 critical tyrosine residue Tyr$_{414}$ to Alanine (Y414A). Two hours after release from the ER, RUSH-synchronized LAMP1^{Y414A} was localized at the plasma membrane whereas LAMP1 wild-type reached LE/Lys. (Figure 2a; Supplemental Movie 3). No fluorescent signal of LAMP1^{Y414A} was detected in intracellular compartments. The appearance and persistence of SBP-EGFP-LAMP1^{Y414A} at the cell surface was confirmed by flow cytometry using anti-GFP immunostaining on nonpermeabilized cells (Figure 2b). Interestingly, LAMP1^{Y414A} and wild-type LAMP1 were not sorted at the Golgi apparatus and exited from the Golgi apparatus in the same tubulovesicular intermediates (Figure 2, c and d; Supplemental Movie 4). TIRF microscopy showed that LAMP1 wild-type and LAMP1^{Y414A} containing carriers fused with the plasma membrane in the same exocytic events indicating that LAMP1 wild-type and LAMP1^{Y414A} have not been sorted after Golgi exit (Figure 2, e–g; Supplemental Movie 5). Consistent with the role of $_{414}$YQTI$_{417}$ motif in the recruitment of AP2 at clathrin-coated pits, SBP-mCherry-LAMP1^{Y414A} was not enriched in punctate structures at the plasma membrane but diffused quickly in the plasma membrane (Figure 2, e–g).

These results show that LAMP1 wild-type and LAMP1^{Y414A} follow the same Golgi-to-plasma membrane transport route. The presence of LAMP1^{Y414A} at the plasma membrane exclusively and the absence of sorting of LAMP1 wild-type and LAMP1^{Y414A} at the Golgi apparatus argue against the existence of a direct Golgi-to-endosome transport route.

LAMP1 and LIMP2 are sorted at the Golgi apparatus

The anterograde transport of several LMPs was then analyzed using the RUSH assay and compared with the trafficking of LAMP1.

In addition to LAMP1, LIMP2, LAMP2, and Lysosomal Acid Phosphatase (LAP) were used as RUSH cargos. LAMP2 and LAP are type I LMPs. LAP is a luminal lysosomal enzyme, synthesized as a membrane bound protein. The luminal domain, which bears its enzymatic activity, is cleaved upon reaching LE/Lys. (Waheed *et al.*, 1988; Braun *et al.*, 1989). LAMP2, LAP, and LIMP2 were retained in the ER in the absence of biotin thanks to the coexpression of an ER-resident hook (Supplemental Figure S3). After the addition of biotin, RUSH-synchronized LAMP2, LAP, and LIMP2 were detected in the Golgi apparatus. Two hours after their release from the ER, they reached LE/Lys. as confirmed by immunostaining of LAMTOR4 (Supplemental Figure S3). The distribution of these proteins at the Golgi apparatus was observed with a higher resolution using a Live-SR module (from Gataca Systems). This system is based on an optically demodulated structured illumination technique and increases the resolution by a factor ≈ 2, leading to a maximum xy resolution of ≈ 120–140 nm at the used acquisition setting (Azuma and Kei, 2015). High-resolution images showed that both LAMP2 and LAP were fully colocalized with LAMP1 in the Golgi apparatus (Supplemental Figures S4, a and b; and S5, a and b). In addition, time-lapse microscopy showed that LAMP2 and LAP exited the Golgi apparatus in the same tubulovesicular carriers as LAMP1 (Supplemental Figures S4, c and d; and S5, c and d; Supplemental Movies 6 and 7), indicating that no sorting of these LMPs occurred at the Golgi apparatus. LAMP2 and LAP were transiently detected at the cell surface by flow cytometry after their synchronous release from the ER (Supplemental Figures S4e and S5e) as previously shown for LAMP1 (Figure 1b). Interestingly, RUSH-synchronized LIMP2 was segregated from LAMP1 at the Golgi apparatus as highlighted by high-resolution microscopy. In addition to a diffuse localization in the Golgi apparatus, similar to LAMP1, LIMP2 was detected in puncta with higher fluorescence intensity (Figure 3, b and c). Segregation of LIMP2 and LAMP1 in the Golgi apparatus was also detected in SUM159 and RPE-1 cells (Supplemental Figure S6). Time-lapse imaging showed that LIMP2 was first diffusely localized at the Golgi apparatus and then enriched in bright puncta (Figure 3, d and e; Supplemental Movie 8). After appearance, these puncta remained associated with the Golgi apparatus for several minutes before leaving it (Figure 3, d and e). LAMP1-containing tubulovesicular carriers and LIMP2-containing vesicular carriers were distinct and described spatially independent Golgi exit routes (Figure 3, f and g; Supplemental Movie 8). Cryo-immuno electron microscopy experiments showed that, 25 min after biotin addition, LAMP1 was distributed in several cisternae of the Golgi stack whereas LIMP2 was segregated in small vesicles apposed to the Golgi cisternae, confirming the segregation between LAMP1 and LIMP2 (Figure 3h). Those LIMP2-positive vesicles appeared to be noncoated and LIMP2 was absent from visible peri-Golgi clathrin-coated vesicles (Figure 3h). We also performed correlative light-electron microscopy (CLEM) experiments, which showed that whereas SBP-mCherry-LAMP1 fluorescence overlaps the entire Golgi stack, SBP-EGFP-LIMP2 bright puncta were localized in regions rich in vesicles with a diameter of 50–70 nm (Figure 3, i–k).

Our data demonstrated that LAMP1, LAMP2, and LAP are not sorted and follow the same transport pathway to the plasma membrane. In contrast, LAMP1 and LIMP2 are segregated at the level of the Golgi complex and leave it in morphologically different carriers.

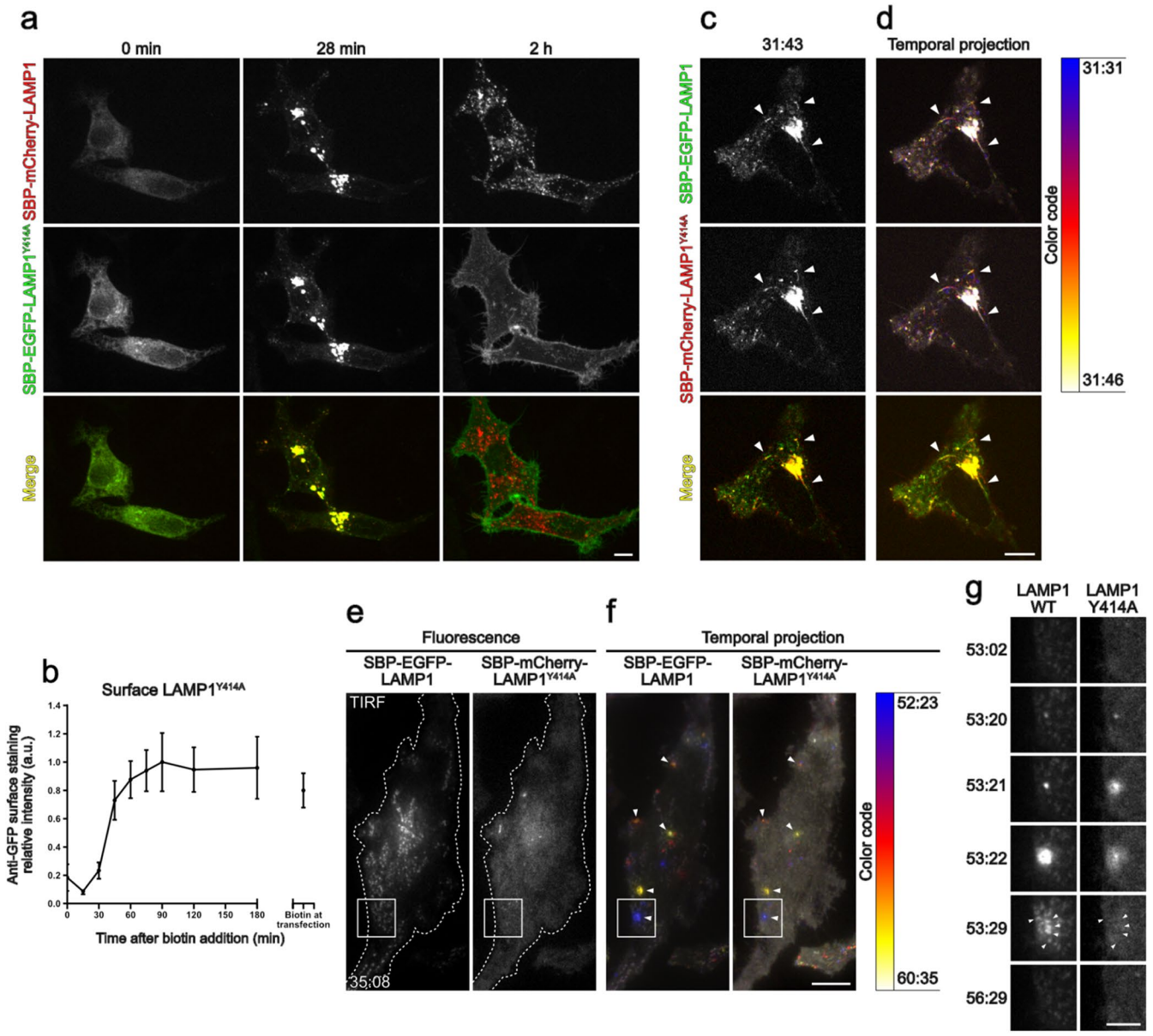

FIGURE 2: LAMP1^{Y414A} is blocked at the cell surface but follows the same Golgi-to-plasma membrane route as LAMP1 wild-type. (a) Living HeLa cells transiently expressing both SBP-mCherry-LAMP1 (WT) and SBP-EGFP-LAMP1^{Y414A} and Streptavidin-KDEL. The same cells were imaged at different times after the addition of biotin. Images correspond to maximum Z projections of several slices acquired with a spinning disk microscope. Scale bar: 10 µm. (b) Flow cytometry quantification of the presence of SBP-EGFP-LAMP1^{Y414A} at the plasma membrane. HeLa cells transiently expressing SBP-EGFP-LAMP1^{Y414A} and Streptavidin-KDEL were incubated with biotin for different times, stained with an anti-GFP antibody without permeabilization. Median anti-GFP intensity of GFP-positive cells normalized to the maximum value is shown, $n = 3$ independent experiments. Error bars: SEM. (c and d) Living HeLa cells transiently expressing both SBP-EGFP-LAMP1 and SBP-mCherry-LAMP1^{Y414A} and Streptavidin-KDEL were acquired every second. Scale bar: 10 µm. (c) Single Z-slice acquired with a spinning-disk microscope at the indicated time after biotin addition. Arrowheads indicate Golgi exit events. (d) Color-coded temporal projections between the two indicated times. (e and f) TIRF images of living HeLa cells transfected as in (c) and acquired every second. Scale bar: 10 µm. (f) Color-coded temporal projections between the indicated times. Arrowheads indicate fusion events with the plasma membrane. (g) Magnified view of boxed areas in (e and f). Arrowheads indicate the retention of LAMP1 retention points in clathrin-coated pits. Scale bar: 5 µm. Time in min:s.

The di-Leucine-like motif of LIMP2 is not involved in its export from the Golgi apparatus

LIMP2 has been suggested to follow a direct Golgi-to-endosome transport pathway (Vega *et al.*, 1991; Obermuller *et al.*, 2002) depending on its di-leucine-like motif ([D/E]XXXL[L/I]; Ogata and Fukuda, 1994), which is involved in binding to AP3 and in its transport to lysosomes (Honing *et al.*, 1998; Le Borgne *et al.*, 1998). The critical Leucine 475 and Isoleucine 476 residues (Figure 3a) of LIMP2 were mutated to Alanine, mutant hereafter named LIMP2^{AA}. At steady state, SBP-mApple-LIMP2^{AA} displayed an increased

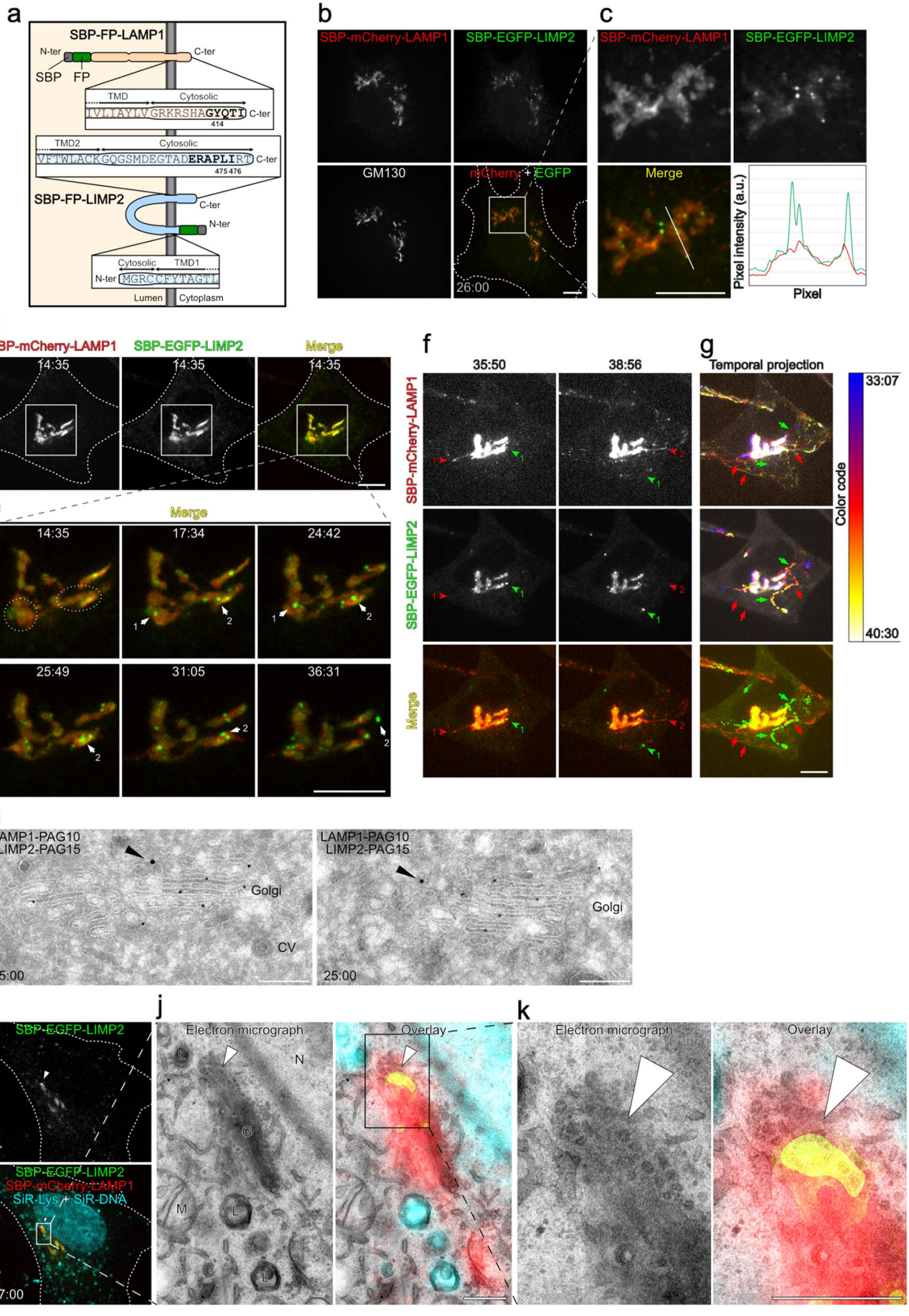
a
SBP-FP-LAMP1
N-ter
C-ter
SBP
FP
TMD
Cytosolic
IVLIAYLVGRKRSHAGYQTI
C-ter
414
TMD2
Cytosolic
VFTWLACKGQGSMDEGTADERAPLIRT
C-ter
475 476
SBP-FP-LIMP2
C-ter
N-ter
Cytosolic
TMD1
N-ter
MGRCCFYTAGTL
Lumen
Cytoplasm
b
SBP-mCherry-LAMP1
SBP-EGFP-LIMP2
GM130
mCherry + EGFP
26:00
c
SBP-mCherry-LAMP1
SBP-EGFP-LIMP2
Merge
Pixel intensity (a.u.)
Pixel
d
SBP-mCherry-LAMP1
SBP-EGFP-LIMP2
Merge
14:35
14:35
14:35
e
Merge
14:35
17:34
24:42
25:49
31:05
36:31
f
35:50
38:56
SBP-mCherry-LAMP1
SBP-EGFP-LIMP2
Merge
g
Temporal projection
33:07
Color code
40:30
h
LAMP1-PAG10
LIMP2-PAG15
Golgi
CV
25:00
LAMP1-PAG10
LIMP2-PAG15
Golgi
25:00
i
SBP-EGFP-LIMP2
SBP-EGFP-LIMP2
SBP-mCherry-LAMP1
SiR-Lys + SiR-DNA
27:00
j
Electron micrograph
Overlay
L
N
G
M
L
L
k
Electron micrograph
Overlay

presence at the plasma membrane compared with wild-type LIMP2 (Figure 4a). However, LIMP2^{AA} reached the same final intracellular compartments as wild-type LIMP2 as highlighted by the condition in which biotin was added at the time of transfection (Figure 4a). The mutation of the [D/E]XXXL[L/I] motif of LIMP2 did not prevent the formation of LIMP2 bright puncta at the Golgi apparatus, LIMP2^{AA} and wild-type LIMP2 being enriched in the same puncta (Figure 4b). LIMP2^{AA} and wild-type LIMP2 left the Golgi apparatus in the same post-Golgi transport intermediates (Figure 4, c and d; Supplemental Movie 9). LIMP2 was shown to be able to dimerize (Conrad *et al.*, 2017). When expressed alone, LIMP2^{AA} and wild-type LIMP2 displayed the same localization as when being coexpressed, ruling out that interaction between the wild-type and the mutant forms of LIMP2 would affect their respective transport route. At steady state, LIMP2^{AA} was present at the plasma membrane and at LE/Lys. whereas wild-type LIMP2 was detected at LE/Lys. only (Supplemental Figure S7, a and b). At the Golgi apparatus, LIMP2^{AA} expressed alone behaved similarly to wild-type LIMP2, with the appearance of bright puncta (Supplemental Figure S7, c and d). Finally, using high-resolution fluorescence microscopy we showed that LIMP2-containing bright puncta did not colocalize with exogenously expressed mCherry-clathrin light chain (Figure 4, e–g).

In conclusion, the clathrin adaptor binding motif [D/E]XXXL[L/I] of LIMP2 is not involved in the segregation of LIMP2 at the Golgi apparatus nor in its export from the Golgi apparatus.

LIMP2 C-terminal cytosolic domain is not involved in its segregation at the Golgi apparatus

We next investigated whether LIMP2 export from the Golgi might depend on another yet unidentified cytosolic signal. As a type III protein, LIMP2 spans the membrane twice and has two cytosolic domains. Its N-terminal cytosolic domain comprises only four residues, including the initiating methionine residue (Figure 3a). We therefore focused on its C-terminal cytosolic domain. Domain swapping experiments between LAMP1 and LIMP2 cytosolic domains were conducted. RUSH chimeras where the LAMP1 cytosolic domain was replaced with the LIMP2 C-terminal cytosolic domain (LAMP1^{LIMP2C}) and the LIMP2 C-terminal cytosolic domain replaced by the LAMP1 cytosolic domain (LIMP2^{LAMP1C}) were generated (Figure 5a). A deletion mutant of LIMP2 missing the whole C-terminal cytosolic domain was also generated (LIMP2$^{\Delta C}$). Among these constructs, only RUSH-synchronized LIMP2^{LAMP1C} and LIMP2$^{\Delta C}$ displayed a punctate localization at the Golgi in contrast to LAMP1^{LIMP2C} (Figure 5b). In conclusion, LIMP2 C-terminal cytosolic domain is neither sufficient nor necessary to induce the enrichment of LMPs in these punctate structures at the Golgi apparatus.

DISCUSSION

Our study demonstrates that human LAMP1 reaches the LE/Lys. after transiting through the plasma membrane, thus following an indirect pathway from the ER to the lysosome. This trafficking route is observed in cells overexpressing RUSH-synchronized LAMP1 as well as at endogenous expression level when the LAMP1 gene is tagged with RUSH-compatible domains. This suggests that the secretory compartments are not overloaded due to high expression, contradicting previous hypotheses (Harter and Mellman, 1992). Mutating LAMP1 YXXΦ cytosolic signal does not change the nature of its post-Golgi carriers, indicating that this motif is not involved in sorting at the level of the Golgi apparatus. Our present data confirm previous results from Chen *et al.* (2017) who used RUSH-synchronized rat LAMP1 and LAMP1^{Y404A}. We show that RUSH-synchronized human wild-type LAMP1 and LAMP1^{Y414A} were fully colocalized in post-Golgi transport intermediates. Chen *et al.* (2017) showed that LAMP1^{Y404A} was addressed from the Golgi apparatus to the plasma membrane in tubulovesicular carriers as rat wild-type LAMP1 does. This rules out the existence of a direct transport pathway from the ER to the LE/Lys. for LAMP1 dependent on its APs binding signal, at least in our experimental conditions or if it does exist, the direct transport is very minor. Pols *et al.* (2013) have shown that LAMP1 and LAMP2 localize in post-Golgi uncoated compartments devoid of cation-independent mannose-6-phosphate receptor (CI-MPR) in several cell lines, including HeLa cells. These structures were positive for the CORVET/HOPS subunit Vps41 as well as for the SNARE VAMP7 and were proposed to mediate direct trafficking to endosomes (Pols *et al.*, 2013). However, we and others (Chen *et al.*, 2017)

FIGURE 3: LAMP1 and LIMP2 are segregated and sorted at the Golgi apparatus. (a) Schematic representations of LAMP1 and LIMP2 topologies, tagging and cytosolic motifs. Clathrin adaptors recruitment signals are shown in bold. FP: fluorescent protein. (b and c) High-resolution images of HeLa cells transiently transfected to express Streptavidin-KDEL, SBP-mCherry-LAMP1, Streptavidin-HA-Endo-KKXX and SBP-EGFP-LIMP2. Cells were incubated with biotin for 26 min, fixed and stained for GM130. The images correspond to maximum Z projection of high-resolution image stacks. Scale bars: 10 µm. (c) Magnified view of the boxed area in (b). Linescan of pixel intensities along the line normalized on the Golgi mean intensity. (d–g) Living HeLa cells transfected to express Streptavidin-KDEL, SBP-mCherry-LAMP1, mini-Ii-Streptavidin and SBP-EGFP-LIMP2 acquired every 2 s. Images correspond to maximum Z projection of spinning-disk stacks acquired at indicated times after biotin addition. Scale bars: 10 µm. (e) Magnified view of the boxed area in (d). Arrows track two puncta from their appearance to their Golgi exit. The dotted ovals highlight the appearance area of the two tracked puncta. (f) Same cells as in (d and e). Red and green arrowheads indicate carriers that exit the Golgi apparatus for SBP-mCherry-LAMP1 and SBP-EGFP-LIMP2, respectively. (g) Color-coded temporal projection between the two indicated times. Arrows track the carriers leaving the Golgi apparatus. Scale bar: 10 µm. (h) Cryo-immuno electron microscopy pictures of HeLa cells transiently expressing Streptavidin-KDEL, SBP-mCherry-LAMP1, Streptavidin-HA-Endo-KKXX and SBP-EGFP-LIMP2. Cells were incubated with biotin for 25 min, fixed and prepared for cryo-immuno electron microscopy. SBP-mCherry-LAMP1 was detected with an anti-mCherry antibody and 10-nm gold particles conjugated to Protein A (PAG10). SBP-EGFP-LIMP2 was detected with an anti-GFP antibody and 15-nm gold particles conjugated to Protein A (PAG15). Arrowheads highlight SBP-EGFP-LIMP2; CV: coated vesicle. Scale bar: 250 nm (i–k) CLEM of SBP-EGFP-LIMP2 and SBP-mCherry-LAMP1. HeLa cells were transfected like in (b and c) and were live stained using SiR-lysosome (SiR-Lys) and SiR-DNA, incubated with biotin for 27 min, fixed, acquired for fluorescence, and then prepared for transmission electron microscopy (TEM). The arrowhead indicates a SBP-EGFP-LIMP2 bright punctum at the Golgi apparatus. (i) Images are confocal spinning-disk Z slices. Scale bar: 10 µm. (j and k) TEM images and fluorescence-EM correlation. The SiR-lysosome staining was used for the correlation. L, lysosome; M, mitochondria; N, nucleus; G, Golgi stack. Scale bar: 1 µm. Time in min:s.

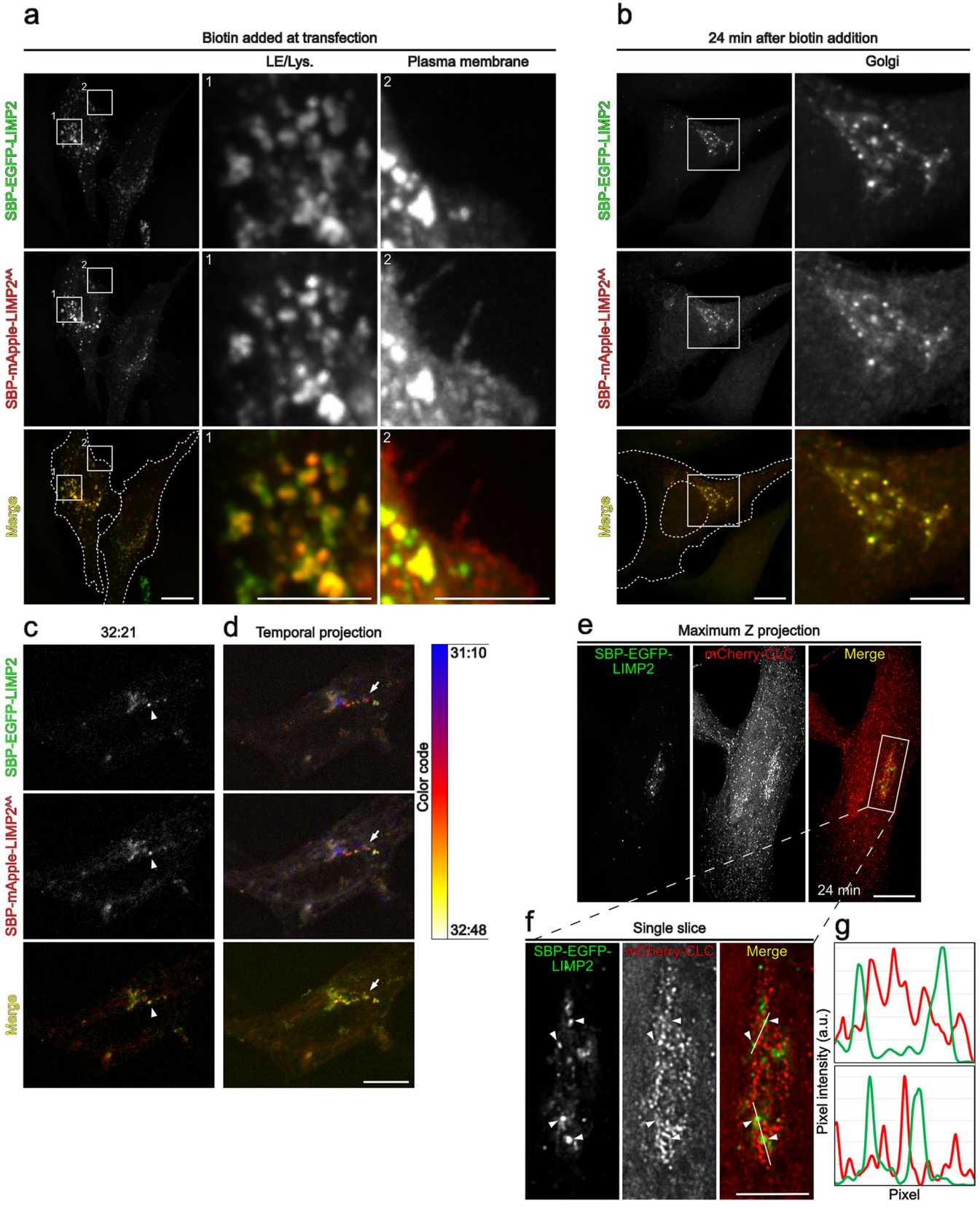

FIGURE 4: LIMP2 [D/E]XXXL[L/I] motif is not involved in its sorting at the Golgi apparatus. (a and b) HeLa cells transiently expressing mini-Ii-Streptavidin, SBP-EGFP-LIMP2 WT, Streptavidin-HA-Endo-KKXX and SBP-mApple-LIMP2^{AA}. Images correspond to maximum Z projection of spinning disk confocal stacks. Scale bars: 10 µm, magnified views: 5 µm. Cells were fixed 24 h after transfection. (b) Cells were incubated with biotin for 24 min and fixed. (c and d) HeLa cells were transfected to express mini-Ii-Streptavidin, SBP-EGFP-LIMP2 WT and SBP-mApple-LIMP2^{AA}. Pictures were acquired every 2 s to follow the Golgi exit events. Scale bar: 10 µm. (c) Arrowheads point out a compartment exiting the

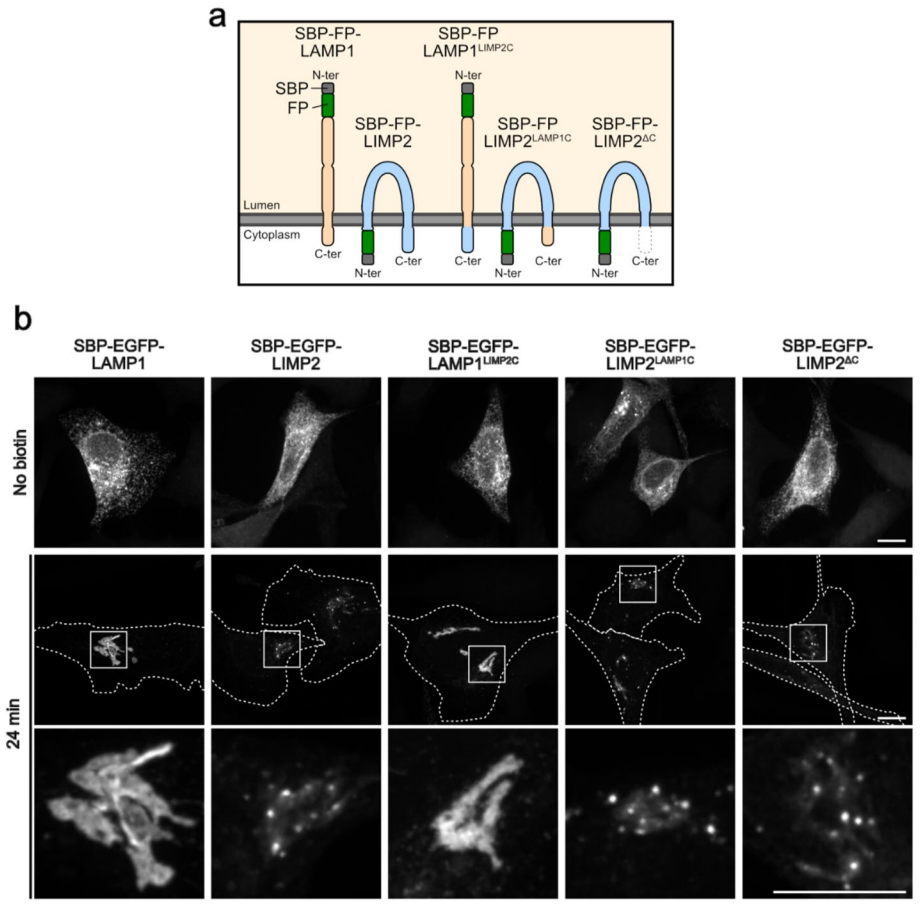

FIGURE 5: LIMP2 C-terminal cytosolic domain is not involved in its sorting at the Golgi apparatus. (a) Schematic representation of the LAMP1/LIMP2 chimeras and LIMP2 deletion mutant. (b) HeLa cells were transfected to express Streptavidin-KDEL (for SBP-EGFP-LAMP1 or SBP-EGFP-LAMP1^{LIMP2C}) or mini-li-Streptavidin (for SBP-EGFP-LIMP2, SBP-EGFP-LIMP2^{LAMP1C} or SBP-EGFP-LIMP2$^{\Delta C}$ treated or not with biotin for 24 min and fixed. Images correspond to maximum Z projection of spinning disk confocal image stacks. Dotted lines indicate cell contour. Bottom panel corresponds to enlargement of the Golgi region boxed in the upper lane. Scale bars: 10 µm.

did not detect such a pathway using the synchronization of the biosynthetic transport of lysosomal membrane, suggesting that either this pathway is insignificant, or that the tagging with SBP prevents its manifestation.

LAMP1 endocytosis and targeting to lysosomes have been shown to be dependent on clathrin and AP2 (Furuno *et al.*, 1989a; Janvier and Bonifacino, 2005; Chen *et al.*, 2017). We showed that when reaching the plasma membrane, LAMP1 is quickly trapped in clathrin-positive areas. The incorporation of LAMP1 in clathrin-coated structures is dependent on its YXXΦ motif. This process is highly dynamic and efficient, explaining why it is difficult to detect endogenous LAMP1 at the cell surface at steady state.

Our data showed that LAMP1, LAMP2, and LAP follow the same transport route from the Golgi apparatus to lysosomes via the plasma membrane, in accordance with previous studies (Braun *et al.*, 1989; Nabi *et al.*, 1991; Obermuller *et al.*, 2002).

As LIMP2 was proposed to follow a direct pathway from the Golgi apparatus to endosomes (Vega *et al.*, 1991; Obermuller *et al.*, 2002), one could expect LIMP2 to be sorted from LAMP1/LAMP2/LAP at the Golgi apparatus. Consistently, although LAMP1 and LIMP2 were colocalized when they reach the Golgi apparatus, LIMP2 then concentrated in punctate structures from which LAMP1 was absent. This result demonstrated that segregation occurs at the level of the Golgi apparatus. Chen *et al.* (2017) have shown sorting of RUSH-synchronized LAMP1 and cation-dependent (CD)-MPR within the Golgi apparatus. Our results suggest that CD-MPR and LIMP2 do not follow the same pathways. Indeed, LIMP2 post-Golgi transport intermediates were not colocalized with exogenously expressed mCherry-clathrin light chain while Mannose-6-phosphate receptors (MPRs) recruit clathrin through binding to Golgi-localized Gamma ear-containing, Arf-binding adaptors (GGAs) for their exit from the Golgi apparatus (Puertollano *et al.*, 2001; Zhu *et al.*, 2001; Doray *et al.*, 2002a; Chen *et al.*, 2017).

Both LAMP1 and LIMP2 recruit AP1 via their cytosolic signals in vitro (Honing *et al.*, 1996; Fujita *et al.*, 1999). LAMP1 has been shown to be present in clathrin-coated vesicles in close proximity of the Golgi apparatus (Honing *et al.*, 1996). However, the depletion of AP1 does not prevent LAMP1 from reaching LE/Lys. (Meyer *et al.*, 2000; Janvier and Bonifacino, 2005; Chen *et al.*, 2017). Here, we show that mutating their APs binding signal does not modify LAMP1 and LIMP2 export from Golgi. In this context, one could wonder whether AP1 is involved in the Golgi exit of these proteins. AP1 also interacts with MPRs and has been proposed to be involved in their export from the Golgi apparatus (Honing *et al.*, 1997; Doray *et al.*, 2002b; Ghosh and Kornfeld, 2003, 2004; Stockli *et al.*, 2004). However, AP1 depletion or knock-sideway (i.e., docking AP1 on mitochondria membranes) does not result in a blockage of MPRs at the Golgi apparatus, but rather in an enrichment of MPRs in endosomes (Meyer *et al.*, 2000; Robinson *et al.*, 2010). This raises the hypothesis that AP1 could be involved in the retrograde endosome-to-Golgi pathway (Meyer *et al.*, 2000; Robinson *et al.*, 2010). Whether AP1 could have such a role for LAMP1 or LIMP2 is an intriguing question, which deserves further investigation. This could bring an explanation for the presence of LAMP1 in compartments positive for Vps41 and VAMP7 near the Golgi apparatus, as observed by Pols *et al.* (2013).

Golgi apparatus. (d) Color-coded temporal projection between the two indicated times. Arrows indicate a track exiting the Golgi apparatus. (e and f) High resolution image of HeLa cells transiently expressing mini-li-Streptavidin, SBP-EGFP-LIMP2 and mCherry-clathrin light chain (CLC). The cells were incubated with biotin for 24 min and fixed. Images correspond to maximum Z projections (e) or single slices (f) of high-resolution image stacks and deconvolved. (e) Scale bar: 10 µm. (f) Arrowheads indicate LIMP2 bright puncta at the Golgi apparatus. Scale bar: 5 µm. (g) Linescans of pixel intensity along the two lines in (f), normalized to the maxima. Time in min:s.

At steady state (1 d after transfection and continuous incubation with biotin), SBP-mApple-LIMP2^{AA} localizes in LE/Lys., as does wild-type LIMP2, but also shows an increased presence at the cell surface (Figure 4a and Supplemental Figure S7, a–b). This could be due to impaired endocytosis secondary to LIMP2AA inability to recruit the endocytic machinery. LIMP2 would reach the plasma membrane after exiting the Golgi apparatus, even though an indirect pathway to LE/Lys. for LIMP2 is in contradiction with previous published data (Vega *et al.*, 1991; Obermuller *et al.*, 2002), or because of LE/Lys. fusion with the plasma membrane. These kinds of fusion events have been described in a multitude of contexts, such as exosome secretion (Kowal *et al.*, 2014), plasma membrane repair (Jimenez and Perez, 2017) or unconventional secretion (Rabouille, 2017). Another possibility would be that LIMP2^{AA} would struggle to orientate to LE/Lys. after reaching endosomes, due to its inability to recruit AP3. Increased surface expression of other LMPs such as LAMP1, LAMP2, and CD63 has been described when AP3 is defective (Dell'Angelica *et al.*, 1999). Unfortunately, our results do not allow to conclude on the transport route of LIMP2 to LE/Lys. after its Golgi exit.

Post-Golgi transport intermediates containing LIMP2 colocalized with vesicular regions close to the Golgi apparatus, as suggested by our immuno EM and CLEM experiments, but are devoid of clathrin. The mechanisms involved in LIMP2 concentration and in the formation of these intermediates require further investigation. Interestingly, LIMP2-containing puncta remain associated with the Golgi apparatus for several minutes before leaving, which could indicate maturation processes might be required for their Golgi exit. As the mutation in the adaptor-binding signal in LIMP2 did not modify its exit from the Golgi apparatus, we investigated whether another motif in its C-terminal cytoplasmic domain could be involved in the formation of LIMP2 post-Golgi transport intermediates. However, the C-terminal cytoplasmic domain of LIMP2 appeared neither sufficient nor essential for the formation of LIMP2 bright puncta and its segregation from LAMP1.

The contribution of LIMP2's biophysical properties and interactions with partners to the formation of these puncta remains unclear. LIMP2 has been shown to be able to dimerize, allowing it to function as a lipid channel (Conrad *et al.*, 2017; Heybrock *et al.*, 2019).The potential role of the dimerization or the lipid-association of LIMP2 in LIMP2 packing within vesicles at the Golgi apparatus remains open. The lysosomal enzyme beta-glucocerebrosidase (βGC) binds LIMP2 in the ER and uses LIMP2 as a sorting receptor for its transport to lysosomes (Reczek *et al.*, 2007). Deletion or mutations of the βGC-binding region in LIMP2 (luminal residues V149-Y163) did not prevent LIMP2 to reach lysosomes (Reczek *et al.*, 2007; Blanz *et al.*, 2010; Neculai *et al.*, 2013). The three-dimensional conformation of this region has also been shown to be pH-sensitive, allowing the release of βGC in the lumen of lysosomes (Reczek *et al.*, 2007; Zachos *et al.*, 2012; Neculai *et al.*, 2013). Mutations of these pH-sensitive luminal residues (H_{150} and H_{171}) did not impair LIMP2 targeting to lysosomes (Zachos *et al.*, 2012). Zhao *et al.* (2014) identified a mannose-6-phosphate (M6P) on LIMP2 and described the formation in vitro of a ternary complex βGC-LIMP2-CI-MPR. However, the biological relevance of this M6P was disputed (Blanz *et al.*, 2010). Indeed, several studies have suggested that both βGC and LIMP2 reach lysosomes in a M6P/MPRs-independent manner (Owada and Neufeld, 1982; Aerts *et al.*, 1988; Blanz *et al.*, 2015). Consistently, we showed by immunofluorescence and electron microscopy that RUSH-synchronized LIMP2-containing vesicles lack clathrin, which could confirm that LIMP2 trafficking is unlikely to be MPR-dependent.

In depth investigation of the molecular players and intrinsic biophysical properties regulating the transport of LIMP2 in a biological context is needed and extends beyond the scope of our study.

MATERIALS AND METHODS

Request a protocol through *Bio-protocol*.

Immunofluorescence and flow cytometry

Cell fixation was performed by incubation in 3% paraformaldehyde (Electron Microscopy Sciences; catalogue no. 15710) for 10 min and permeabilized by incubation in 0.5 g/L saponin in phosphate-buffered saline (PBS) supplemented with 2 g/L bovine serum albumin. Primary antibodies used in this study were anti-GM130 (BD Transduction Laboratories; catalogue no. 610823; dilution 1:1000), anti-giantin (clone TA10; recombinant antibody facility of Institut Curie, Paris, France), anti-LAMTOR4 (Cell Signaling Technology; catalogue no. 13140 dilution 1:1000), anti-PDI isoform A3 (Sigma-Aldrich; catalogue no. AMAB90988; 1:250). Fluorochrome conjugated secondary antibodies were purchased from Jackson ImmunoResearch. Coverslips were mounted in Mowiol containing DAPI. In Supplemental Figure S7, cells were stained with HCS CellMask Blue Stain (Thermo Fisher Scientific; catalogue no. H32720; diluted at 1:5000 in the mounting medium). For cell surface staining, cells were transferred in ice-cold PBS and incubated with an Alexa Fluor 647-coupled anti-GFP antibody (BD Pharmingen; catalogue no. 565197; dilution 1:150), for 40 min before fixation with 2% paraformaldehyde. Signal intensity was analyzed by flow cytometry using a BD Accuri C6 or a Miltenyi MACSQuant10 cytometer. Median anti-GFP intensity of GFP-positive cells normalized to the maximum value is depicted on the graph.

Cryo-immuno-electron microscopy

Cells were fixed with 2% paraformaldehyde and 0.2% glutaraldehyde in 0.1M sodium phosphate buffer, pH 7.4. After washing in PBS/Glycine 0,02M, cells were pelleted by centrifugation, embedded in 12% gelatin, cooled in ice and cut into 5-mm3 blocks. The blocks were infused overnight with 2.3 M sucrose at 4°C, frozen in liquid nitrogen and stored until cryo-ultramicrotomy. Sections of 80 nm were cut with a diamond knife (Diatome) at –112°C using Leica EM-UC7. Ultrathin sections were picked up in a mix of 1.8% methylcellulose and 2.3 M sucrose (1:1) according to (Liou *et al.*, 1996) and transferred to formvar carbon-coated copper grids. Double immunolabeling was performed as described before (Slot *et al.*, 1991) with optimal combination of gold particle sizes and sequence of antibodies. Cryosections were first incubated with rabbit polyclonal anti-GFP antibody (invitrogen) followed by protein A gold-15 nm (Slot and Geuze, 1985). After postfixation with 1% glutaraldehyde in PBS, cryosections were incubated with a rabbit polyclonal anti-mCherry antibody (antibody facility of the Institut Curie) followed by protein A gold-10 nm. After labelling, the sections were treated with 1% glutaraldehyde, counterstained with uranyl acetate, and embedded in methyl cellulose uranylacetate (Slot *et al.*, 1991). Grids were observed on a Tecnai G2 spirit (FEI Company) equipped with a 4-k CCD camera (Quemesa, Olympus).

Correlative light-electron microscopy (CLEM)

HeLa cells expressing RUSH cargos were live-stained for 1 h with SiR-lysosome (Spirochrome) and SiR-DNA (Spirochrome) at 1 μM each. The cells were then incubated with biotin for 27 min and fixed with 3% paraformaldehyde (Electron Microscopy Sciences; catalogue no. 15710) for 10 min. Fluorescence images were then acquired using an Eclipse 80i microscope (Nikon) equipped with a CSU-X1 Yokogawa spinning-disk head and an Ultra897 iXon EMCCD camera (Andor). The cells were then postfixed with glutaraldehyde 2.5% in cacodylate buffer 0,1 M, pH 7.2 and then with 1% (wt/vol) OsO_4 supplemented with 1.5% (wt/vol) potassium ferrocyanide,

dehydrated in increasing concentration of ethanol (50, 70, 90, 96, and 100%). Cells were embedded in epon 812 (TAAB Laboratories Equipment) and processed for serial ultrathin sectioning with a Reichert Ultracut S ultramicrotome (Leica). Sections were counterstained with uranyl acetate and lead citrate, and observed with a Transmission Electron Microscope (TEM; Tecnai G2 Spirit; FEI) equipped with a Quemesa 4k CCD camera (Olympus).

Fluorescence and EM images were correlated based on the SiR-lysosome staining and using the eC-CLEM software (Paul-Gilloteaux *et al.*, 2017).

RUSH constructs and other plasmids

All RUSH constructs were expressed using bicistronic plasmids coding for both SBP-FP-tagged LMP and the hook. SBP-FP-LAMP1 (LAMP1 sequence from NM_005561.3 generated from cDNA from GE Dharmacon, Clone ID 3872778), its mutants, SBP-FP-LAMP2 (isoform B, nucleotide sequence NM_013995.2, generated from a plasmid kindly given by Y. Baudat, Sanofi R&D Centre, Vitry sur Seine, France) and SBP-FP-LAP (isoform 1, nucleotide sequence NM_001357016.1 generated from a cDNA from GE Dharmacon, Clone ID 30332133) were used with the luminal hook Streptavidin-KDEL (Boncompain *et al.*, 2012). SBP-FP-LIMP2 (isoform 1, nucleotide sequence NM_005506.3, generated from cDNA from GE Dharmacon, Clone ID 3872778) and its mutants were cytosolically tagged and coexpressed with either Streptavidin-HA-Endo-KKXX or Mini-Ii-streptavidin. Streptavidin-HA-Endo-KKXX consists in the fusion of streptavidin to the HA-tag, the endocytic signal of LAMP1 (AGYQTI) and the COPI recruitment signal of the *Saccharomyces cerevisiae* WBP1 (KKTN). Mini-Ii-streptavidin is composed of the sequence coding for the 46 first amino acids of human CD74/Ii upstream of Streptavidin. All plasmids generated for the present study were verified by sequencing. The EGFP-RAB6 plasmid was a gift from Jamie White (White *et al.*, 1999). The mCherry-clathrin light chain plasmid was a gift from Guillaume Montagnac (Gustave Roussy, Villejuif, France).

Cells culture, transfection, and RUSH assay

HeLa cells were grown at 37°C with 5% CO_2 in DMEM, high glucose, GlutaMAX (Thermo Fischer Scientific) supplemented with 10% fetal calf serum (FCS; Biosera), 1 mM sodium pyruvate (Thermo Fischer Scientific) and 100 U/mL penicillin and streptomycin (Thermo Fischer Scientific). SUM159 cells were cultured in DMEM/F-12 GlutaMAX (GIBCO), supplemented with 5% FCS (Biosera), penicillin-streptomycin (500 µg/ml; GIBCO), hydrocortisone (1 µg/ml; Sigma-Aldrich), insulin (5 µg/ml; Sigma-Aldrich), and 10 mM HEPES (GIBCO). RPE-1 cells were cultured in DMEM/F-12 GlutaMAX (GIBCO), supplemented with 10% FCS (Biosera), penicillin-streptomycin (500 µg/ml; GIBCO). HeLa cells were transfected 24 h before fixation or observation using calcium phosphate method as previously described (Jordan *et al.*, 1996). SUM159 and RPE-1 cells were transfected using JetPrime (Polyplus). To release RUSH cargos, D-biotin (Sigma-Aldrich; catalogue no. B4501) was added to the culture medium at a final concentration of 80 µM.

Genome editing of LAMP1

The sequence of the gRNA targeting the exon 2 of human LAMP1 was 5′-AACGGGACCGCGTGCATAA-3′ downstream of a U6 promoter and upstream of a gRNA scaffold as previously described in (Mali *et al.*, 2013) and has been inserted in a pCRII vector (Thermo Fisher Scientific). The gRNA coding plasmid was cotransfected with a plasmid coding for hCas9 (hCas9 was a gift from George Church (Addgene plasmid # 41815; http://n2t.net/addgene:41815; RRID:Addgene_41815), a plasmid bearing puromycin resistance (pIRES-puromycin from Clonetch; to enrich for transfected cells), the donor plasmid. The donor plasmid was constructed by gene synthesis (Geneart, Thermo Fisher Scientific) of the left and right homology arms (800 bp each) and insertion between the two arms of the cassette SBP-mCherry. Please note that we reconstructed in the donor plasmid the signal peptide of LAMP1, which is coded by part of the exon1 and exon 2 (see Supplemental Figure S2a). SUM159 cells were transfected using JetPrime (Polyplus) following manufacturer's instructions. Twenty-four hour post-transfection puromycin at 5 µg/ml was added for 1 d only. After expansion, clones were obtained by limiting dilutions.

For characterization, the genomic DNA of the clones was extracted (NucleoTissue kit from Macherey-Nagel) from the engineered SBP-mcherry-LAMP1^{EN} knock-in cell lines, and then PCR genotyping was performed to validate the genomic DNA sequences (1 kb upstream of gRNA cutting site forward primer 5′-GCACGGATTC-CAGTGGTGGCA-3′ and 1kb downstream reverse primer 5′-ATG-GTTGGTTGACATGCAATGCAAACA-3′). The genomic sequences of the edited allele in the junction of right and left homologous arms were edited as expected. PCR using forward primer 5′-AAAACC-CCGTCGCTACTAAAAACAGAA-3′, 5′-AATTCCTGCAGGTGGTT-CACGTTGACCTTGTGG-3′, 5′-aattcctgcaggTGGTTCACGTTGACC-TTGTGG-3′, and the reverse primer 5′-GGAAAATGTTCATGATGAA-CAGTGAGG-3′ were used to check the insertion of SBP-mCherry. The genomic DNA sequences of SBP-mCherry CRISPR-Cas9 knock-in were coherent with the expected sequence in the gRNA cutting region of LAMP1.

Fluorescence image acquisition and analysis

Widefield microscopy images were acquired using a Leica DM6000 equipped microscope with a CoolSnap HQ2 (Photometrics) CCD camera. Confocal images of fixed cells were acquired with an Eclipse Ti-E microscope (Nikon) equipped with a CSU-X1 Yokogawa spinning-disk head and a Prime 95B sCMOS camera (Photometrics). High-resolution images were acquired with this same set-up complemented with a Live-SR super-resolution module (Gataca Systems; Roth and Heintzmann, 2016). This device, based on an optically demodulated structured illumination technique, increases the resolution by a factor ≈ 2, leading to a maximum xy resolution of ≈ 120 nm at 480 nm and ≈ 140 nm at 561 nm (Azuma and Kei, 2015). For time-lapse imaging, cells were transferred in the CO_2-independent Leibovitz's medium (Thermo Fischer Scientific) and were acquired at 37°C in a thermostat-controlled chamber. Confocal live-cell images were acquired with an Eclipse 80i microscope (Nikon) equipped with a CSU-X1 Yokogawa spinning-disk head and an Ultra897 iXon EMCCD camera (Andor). TIRF live-cell images were acquired with an Eclipse Ti-E microscope (Nikon) equipped with a TIRF module (Nikon), a 100x CFI Apo TIRF objective and an Evolve EMCCD camera (Photometrics). All acquisitions were driven by the MetaMorph software (Molecular Devices). Pixel intensity linescans, kymographs (Figure 1g) and temporal projections were performed thanks to Fiji software (Schindelin *et al.*, 2012) built-in functions *Plot Profile*, *Multi Kymograph* and *Temporal-Color Code*, respectively.

Declaration of interests

J.E. and E.V. are Sanofi employees and may hold shares and/or stock options in the company.

ACKNOWLEDGMENTS

The authors acknowledge the Cell and Tissue Imaging Platform (PICT-IBiSA) of Institut Curie – CNRS UMR144 and the Nikon Imaging Centre at Institut Curie – CNRS, members of the national

infrastructure France-BioImaging supported by the French National Research Agency (ANR-10-INBS-04) and the recombinant antibody facility, Institut Curie. We also thank Yves Baudat for his input and for providing the plasmid coding for LAMP2B. The work in FP lab work was supported by Labex Cell(n)Scale (ANR-10-LBX-0038 part of the IDEX PSL no. ANR-10- IDEX-0001-02, by the Agence Nationale De La Recherche grants ANR-22-CE14-0066-01, ANR-20-CE14-0017-02, ANR-19-CE13-0006-03, and ANR-19-CE13-0002-03, and by the Fondation pour la Recherche Médicale (EQU201903007925). The grant ANR-20-CE13-0012-01 from Agence Nationale de la Recherche has been attributed to G.B. FDT201805005670 has been attributed to J.E. by the Fondation pour la Recherche Médicale. This work was financially supported by SANOFI (Collaboration agreement SANOFI/Institut Curie/UPMC/CNRS). J.E. was supported by a CIFRE fellowship (N°2015/0313) funded in part by the National Association for Research and Technology (ANRT) on behalf of the French Ministry of Education and Research, and in part by SANOFI. Y.L.L. has been granted with ARC DOC4 from the Fondation ARC pour la Recherche sur le Cancer.

REFERENCES

Aerts JM, Heikoop J, van Weely S, Donker-Koopman WE, Barranger JA, Tager JM, Schram AW (1988). Characterization of glucocerebrosidase in peripheral blood cells and cultured blastoid cells. Exp Cell Res 177, 391–398.

Akasaki K, Michihara A, Mibuka K, Fujiwara Y, Tsuji H (1995). Biosynthetic transport of a major lysosomal membrane glycoprotein, lamp-1: convergence of biosynthetic and endocytic pathways occurs at three distinctive points. Exp Cell Res 220, 464–473.

Azuma T, Kei T (2015). Super-resolution spinning-disk confocal microscopy using optical photon reassignment. Opt Express 23, 15003–15011.

Blanz J, Groth J, Zachos C, Wehling C, Saftig P, Schwake M (2010). Disease-causing mutations within the lysosomal integral membrane protein type 2 (LIMP-2) reveal the nature of binding to its ligand beta-glucocerebrosidase. Hum Mol Genet 19, 563–572.

Blanz J, Zunke F, Markmann S, Damme M, Braulke T, Saftig P, Schwake M (2015). Mannose 6-phosphate-independent lysosomal sorting of LIMP-2. Traffic 16, 1127–1136.

Boncompain G, Divoux S, Gareil N, de Forges H, Lescure A, Latreche L, Mercanti V, Jollivet F, Raposo G, Perez F (2012). Synchronization of secretory protein traffic in populations of cells. Nat Methods 9, 493–498.

Braulke T, Bonifacino JS (2009). Sorting of lysosomal proteins. Biochim Biophys Acta 1793, 605–614.

Braun M, Waheed A, von Figura K (1989). Lysosomal acid phosphatase is transported to lysosomes via the cell surface. EMBO J 8, 3633–3640.

Chen Y, Gershlick DC, Park SY, Bonifacino JS (2017). Segregation in the Golgi complex precedes export of endolysosomal proteins in distinct transport carriers. J Cell Biol 216, 4141–4151.

Conrad KS, Cheng TW, Ysselstein D, Heybrock S, Hoth LR, Chrunyk BA, Am Ende CW, Krainc D, Schwake M, Saftig P, *et al.* (2017). Lysosomal integral membrane protein-2 as a phospholipid receptor revealed by biophysical and cellular studies. Nat Commun 8, 1908.

Cook NR, Row PE, Davidson HW (2004). Lysosome associated membrane protein 1 (Lamp1) traffics directly from the TGN to early endosomes. Traffic 5, 685–699.

Dell'Angelica EC, Shotelersuk V, Aguilar RC, Gahl WA, Bonifacino JS (1999). Altered trafficking of lysosomal proteins in Hermansky-Pudlak syndrome due to mutations in the beta 3A subunit of the AP-3 adaptor. Mol Cell 3, 11–21.

Doray B, Bruns K, Ghosh P, Kornfeld S (2002a). Interaction of the cation-dependent mannose 6-phosphate receptor with GGA proteins. J Biol Chem 277, 18477–18482.

Doray B, Ghosh P, Griffith J, Geuze HJ, Kornfeld S (2002b). Cooperation of GGAs and AP-1 in packaging MPRs at the trans-Golgi network. Science 297, 1700–1703.

Fourriere L, Kasri A, Gareil N, Bardin S, Bousquet H, Pereira D, Perez F, Goud B, Boncompain G, Miserey-Lenkei S (2019). RAB6 and microtubules restrict protein secretion to focal adhesions. J Cell Biol 218, 2215–2231.

Fujita H, Saeki M, Yasunaga K, Ueda T, Imoto T, Himeno M (1999). In vitro binding study of adaptor protein complex (AP-1) to lysosomal targeting motif (LI-motif). Biochem Biophys Res Commun 255, 54–58.

Furuno K, Ishikawa T, Akasaki K, Yano S, Tanaka Y, Yamaguchi Y, Tsuji H, Himeno M, Kato K (1989a). Morphological localization of a major lysosomal membrane glycoprotein in the endocytic membrane system. J Biochem 106, 708–716.

Furuno K, Yano S, Akasaki K, Tanaka Y, Yamaguchi Y, Tsuji H, Himeno M, Kato K (1989b). Biochemical analysis of the movement of a major lysosomal membrane glycoprotein in the endocytic membrane system. J Biochem 106, 717–722.

Ghosh P, Kornfeld S (2003). AP-1 binding to sorting signals and release from clathrin-coated vesicles is regulated by phosphorylation. J Cell Biol 160, 699–708.

Ghosh P, Kornfeld S (2004). The cytoplasmic tail of the cation-independent mannose 6-phosphate receptor contains four binding sites for AP-1. Arch Biochem Biophys 426, 225–230.

Girod A, Storrie B, Simpson JC, Johannes L, Goud B, Roberts LM, Lord JM, Nilsson T, Pepperkok R (1999). Evidence for a COP-I-independent transport route from the Golgi complex to the endoplasmic reticulum. Nat Cell Biol 1, 423–430.

Green SA, Zimmer KP, Griffiths G, Mellman I (1987). Kinetics of intracellular transport and sorting of lysosomal membrane and plasma membrane proteins. J Cell Biol 105, 1227–1240.

Grigoriev I, Splinter D, Keijzer N, Wulf PS, Demmers J, Ohtsuka T, Modesti M, Maly IV, Grosveld F, Hoogenraad CC, Akhmanova A (2007). Rab6 regulates transport and targeting of exocytotic carriers. Dev Cell 13, 305–314.

Grigoriev I, Yu KL, Martinez-Sanchez E, Serra-Marques A, Smal I, Meijering E, Demmers J, Peranen J, Pasterkamp RJ, van der Sluijs P, *et al.* (2011). Rab6, Rab8, and MICAL3 cooperate in controlling docking and fusion of exocytotic carriers. Curr Biol 21, 967–974.

Guarnieri FG, Arterburn LM, Penno MB, Cha Y, August JT (1993). The motif Tyr-X-X-hydrophobic residue mediates lysosomal membrane targeting of lysosome-associated membrane protein 1. J Biol Chem 268, 1941–1946.

Harter C, Mellman I (1992). Transport of the lysosomal membrane glycoprotein lgp120 (lgp-A) to lysosomes does not require appearance on the plasma membrane. J Cell Biol 117, 311–325.

Heybrock S, Kanerva K, Meng Y, Ing C, Liang A, Xiong ZJ, Weng X, Ah Kim Y, Collins R, Trimble W, *et al.* (2019). Lysosomal integral membrane protein-2 (LIMP-2/SCARB2) is involved in lysosomal cholesterol export. Nat Commun 10, 3521.

Honing S, Hunziker W (1995). Cytoplasmic determinants involved in direct lysosomal sorting, endocytosis, and basolateral targeting of rat lgp120 (lamp-I) in MDCK cells. J Cell Biol 128, 321–332.

Honing S, Griffith J, Geuze HJ, Hunziker W (1996). The tyrosine-based lysosomal targeting signal in lamp-1 mediates sorting into Golgi-derived clathrin-coated vesicles. EMBO J 15, 5230–5239.

Honing S, Sosa M, Hille-Rehfeld A, von Figura K (1997). The 46-kDa mannose 6-phosphate receptor contains multiple binding sites for clathrin adaptors. J Biol Chem 272, 19884–19890.

Honing S, Sandoval IV, von Figura K (1998). A di-leucine-based motif in the cytoplasmic tail of LIMP-II and tyrosinase mediates selective binding of AP-3. EMBO J 17, 1304–1314.

Hunziker W, Harter C, Matter K, Mellman I (1991). Basolateral sorting in MDCK cells requires a distinct cytoplasmic domain determinant. Cell 66, 907–920.

Janvier K, Bonifacino JS (2005). Role of the endocytic machinery in the sorting of lysosome-associated membrane proteins. Mol Biol Cell 16, 4231–4242.

Janvier K, Kato Y, Boehm M, Rose JR, Martina JA, Kim BY, Venkatesan S, Bonifacino JS (2003). Recognition of dileucine-based sorting signals from HIV-1 Nef and LIMP-II by the AP-1 gamma-sigma1 and AP-3 delta-sigma3 hemicomplexes. J Cell Biol 163, 1281–1290.

Jimenez AJ, Perez F (2017). Plasma membrane repair: the adaptable cell life-insurance. Curr Opin Cell Biol 47, 99–107.

Jordan M, Schallhorn A, Wurm FM (1996). Transfecting mammalian cells: optimization of critical parameters affecting calcium-phosphate precipitate formation. Nucleic Acids Res 24, 596–601.

Kowal J, Tkach M, Thery C (2014). Biogenesis and secretion of exosomes. Curr Opin Cell Biol 29, 116–125.

Kuronita T, Eskelinen EL, Fujita H, Saftig P, Himeno M, Tanaka Y (2002). A role for the lysosomal membrane protein LGP85 in the biogenesis and maintenance of endosomal and lysosomal morphology. J Cell Sci 115, 4117–4131.

Le Borgne R, Alconada A, Bauer U, Hoflack B (1998). The mammalian AP-3 adaptor-like complex mediates the intracellular transport of lysosomal membrane glycoproteins. J Biol Chem 273, 29451–29461.
Liou W, Geuze HJ, Slot JW (1996). Improving structural integrity of cryosections for immunogold labeling. Histochem Cell Biol 106, 41–58.
Lippincott-Schwartz J, Fambrough DM (1986). Lysosomal membrane dynamics: structure and interorganellar movement of a major lysosomal membrane glycoprotein. J Cell Biol 102, 1593–1605.
Lippincott-Schwartz J, Fambrough DM (1987). Cycling of the integral membrane glycoprotein, LEP100, between plasma membrane and lysosomes: kinetic and morphological analysis. Cell 49, 669–677.
Mali P, Yang L, Esvelt KM, Aach J, Guell M, DiCarlo JE, Norville JE, Church GM (2013). RNA-guided human genome engineering via Cas9. Science 339, 823–826.
Mattera R, Boehm M, Chaudhuri R, Prabhu Y, Bonifacino JS (2011). Conservation and diversification of dileucine signal recognition by adaptor protein (AP) complex variants. J Biol Chem 286, 2022–2030.
Meyer C, Zizioli D, Lausmann S, Eskelinen EL, Hamann J, Saftig P, von Figura K, Schu P (2000). mu1A-adaptin-deficient mice: lethality, loss of AP-1 binding and rerouting of mannose 6-phosphate receptors. EMBO J 19, 2193–2203.
Miserey-Lenkei S, Chalancon G, Bardin S, Formstecher E, Goud B, Echard A (2010). Rab and actomyosin-dependent fission of transport vesicles at the Golgi complex. Nat Cell Biol 12, 645–654.
Miserey-Lenkei S, Bousquet H, Pylypenko O, Bardin S, Dimitrov A, Bressanelli G, Bonifay R, Fraisier V, Guillou C, Bougeret C, *et al*. (2017). Coupling fission and exit of RAB6 vesicles at Golgi hotspots through kinesin-myosin interactions. Nat Commun 8, 1254.
Nabi IR, Bivic AL, Fambrough D, Rodriguez-Boulan E (1991). An endogenous MDCK lysosomal membrane glycoprotein is targeted basolaterally before delivery to lysosomes. J Cell Biol 115, 1573–1584.
Neculai D, Schwake M, Ravichandran M, Zunke F, Collins RF, Peters J, Neculai M, Plumb J, Loppnau P, Pizarro JC, *et al*. (2013). Structure of LIMP-2 provides functional insights with implications for SR-BI and CD36. Nature 504, 172–176.
Obermuller S, Kiecke C, von Figura K, Honing S (2002). The tyrosine motifs of Lamp 1 and LAP determine their direct and indirect targeting to lysosomes. J Cell Sci 115, 185–194.
Ogata S, Fukuda M (1994). Lysosomal targeting of Limp II membrane glycoprotein requires a novel Leu-Ile motif at a particular position in its cytoplasmic tail. J Biol Chem 269, 5210–5217.
Ohno H, Stewart J, Fournier MC, Bosshart H, Rhee I, Miyatake S, Saito T, Gallusser A, Kirchhausen T, Bonifacino JS (1995). Interaction of tyrosine-based sorting signals with clathrin-associated proteins. Science 269, 1872–1875.
Ohno H, Fournier MC, Poy G, Bonifacino JS (1996). Structural determinants of interaction of tyrosine-based sorting signals with the adaptor medium chains. J Biol Chem 271, 29009–29015.
Owada M, Neufeld EF (1982). Is there a mechanism for introducing acid hydrolases into liver lysosomes that is independent of mannose 6-phosphate recognition? Evidence from I-cell disease. Biochem Biophys Res Commun 105, 814–820.
Patwardhan A, Bardin S, Miserey-Lenkei S, Larue L, Goud B, Raposo G, Delevoye C (2017). Routing of the RAB6 secretory pathway towards the lysosome related organelle of melanocytes. Nat Commun 8, 15835.
Paul-Gilloteaux P, Heiligenstein X, Belle M, Domart MC, Larijani B, Collinson L, Raposo G, Salamero J (2017). eC-CLEM: flexible multidimensional registration software for correlative microscopies. Nat Methods 14, 102–103.
Peden AA, Oorschot V, Hesser BA, Austin CD, Scheller RH, Klumperman J (2004). Localization of the AP-3 adaptor complex defines a novel endosomal exit site for lysosomal membrane proteins. J Cell Biol 164, 1065–1076.
Pereira C, Stalder D, Anderson GSF, Shun-Shion AS, Houghton J, Antrobus R, Chapman MA, Fazakerley DJ, Gershlick DC (2023). The exocyst complex is an essential component of the mammalian constitutive secretory pathway. J Cell Biol 222, e202205137.
Pols MS, van Meel E, Oorschot V, ten Brink C, Fukuda M, Swetha MG, Mayor S, Klumperman J (2013). hVps41 and VAMP7 function in direct TGN to late endosome transport of lysosomal membrane proteins. Nat Commun 4, 1361.
Puertollano R, Aguilar RC, Gorshkova I, Crouch RJ, Bonifacino JS (2001). Sorting of mannose 6-phosphate receptors mediated by the GGAs. Science 292, 1712–1716.
Rabouille C (2017). Pathways of unconventional protein secretion. Trends Cell Biol 27, 230–240.
Reczek D, Schwake M, Schroder J, Hughes H, Blanz J, Jin X, Brondyk W, Van Patten S, Edmunds T, Saftig P (2007). LIMP-2 is a receptor for lysosomal mannose-6-phosphate-independent targeting of beta-glucocerebrosidase. Cell 131, 770–783.
Robinson MS (2004). Adaptable adaptors for coated vesicles. Trends Cell Biol 14, 167–174.
Robinson MS, Sahlender DA, Foster SD (2010). Rapid inactivation of proteins by rapamycin-induced rerouting to mitochondria. Dev Cell 18, 324–331.
Roth S, Heintzmann R (2016). Optical photon reassignment with increased axial resolution by structured illumination. Methods Appl Fluoresc 4, 045005.
Sandoval IV, Bakke O (1994). Targeting of membrane proteins to endosomes and lysosomes. Trends Cell Biol 4, 292–297.
Sandoval IV, Martinez-Arca S, Valdueza J, Palacios S, Holman GD (2000). Distinct reading of different structural determinants modulates the dileucine-mediated transport steps of the lysosomal membrane protein LIMPII and the insulin-sensitive glucose transporter GLUT4. J Biol Chem 275, 39874–39885.
Schindelin J, Arganda-Carreras I, Frise E, Kaynig V, Longair M, Pietzsch T, Preibisch S, Rueden C, Saalfeld S, Schmid B, *et al*. (2012). Fiji: an open-source platform for biological-image analysis. Nat Methods 9, 676–682.
Slot JW, Geuze HJ (1985). A new method of preparing gold probes for multiple-labeling cytochemistry. Eur J Cell Biol 38, 87–93.
Slot JW, Geuze HJ, Gigengack S, Lienhard GE, James DE (1991). Immunolocalization of the insulin regulatable glucose transporter in brown adipose tissue of the rat. J Cell Biol 113, 123–135.
Stockli J, Honing S, Rohrer J (2004). The acidic cluster of the CK2 site of the cation-dependent mannose 6-phosphate receptor (CD-MPR) but not its phosphorylation is required for GGA1 and AP-1 binding. J Biol Chem 279, 23542–23549.
Tabuchi N, Akasaki K, Tsuji H (2000). Two acidic amino acid residues, Asp(470) and Glu(471), contained in the carboxyl cytoplasmic tail of a major lysosomal membrane protein, LGP85/LIMP II, are important for its accumulation in secondary lysosomes. Biochem Biophys Res Commun 270, 557–563.
Vega MA, Rodriguez F, Segui B, Cales C, Alcalde J, Sandoval IV (1991). Targeting of lysosomal integral membrane protein LIMP II. The tyrosine-lacking carboxyl cytoplasmic tail of LIMP II is sufficient for direct targeting to lysosomes. J Biol Chem 266, 16269–16272.
Waheed A, Gottschalk S, Hille A, Krentler C, Pohlmann R, Braulke T, Hauser H, Geuze H, von Figura K (1988). Human lysosomal acid phosphatase is transported as a transmembrane protein to lysosomes in transfected baby hamster kidney cells. EMBO J 7, 2351–2358.
White J, Johannes L, Mallard F, Girod A, Grill S, Reinsch S, Keller P, Tzschaschel B, Echard A, Goud B, Stelzer EH (1999). Rab6 coordinates a novel Golgi to ER retrograde transport pathway in live cells. J Cell Biol 147, 743–760.
Williams MA, Fukuda M (1990). Accumulation of membrane glycoproteins in lysosomes requires a tyrosine residue at a particular position in the cytoplasmic tail. J Cell Biol 111, 955–966.
Zachos C, Blanz J, Saftig P, Schwake M (2012). A critical histidine residue within LIMP-2 mediates pH sensitive binding to its ligand beta-glucocerebrosidase. Traffic 13, 1113–1123.
Zhao Y, Ren J, Padilla-Parra S, Fry EE, Stuart DI (2014). Lysosome sorting of beta-glucocerebrosidase by LIMP-2 is targeted by the mannose 6-phosphate receptor. Nat Commun 5, 4321.
Zhu Y, Doray B, Poussu A, Lehto VP, Kornfeld S (2001). Binding of GGA2 to the lysosomal enzyme sorting motif of the mannose 6-phosphate receptor. Science 292, 1716–1718.